

## STUDY OF AIR POLLUTION BY SCREEN 3 MODEL

<sup>1</sup> Department of Engineering and Management, Faculty of Engineering Hunedoara, University Politehnica Timisoara, Hunedoara, ROMANIA

**Abstract:** In this study, the Screen 3 model is used to quantitatively estimate the PM concentration at ground level in the case of a point source emissions over 11 months of the 2019 year. Results are presented versus the distance downwind from the source of 50 km. The influence of the plume rise mechanism (buoyant and momentum) is correlated with the estimated maximum PM concentration. This study presents quantitative results obtained by the Screen 3 model in terms of PM concentration variations estimated at ground level after a point source emission during 11 months over the year 2019. Initial emission parameters were classified in four seasons (winter, spring, summer, and autumn) including the months in which the experimental measurements were made. The model was completed with meteorological data measured by an air monitoring station located near the point emission source.

**Keywords:** point source, particulate matter, air dispersion, Screen 3 model

### 1. INTRODUCTION

The United States Environmental Protection Agency (US EPA) developed the Screen 3 model to estimate the pollutant concentration from air-dispersed Gaussian plumes emitted by point, area, volume, or flare sources [1, 2]. Screen View (Lakes Environmental) is a user-friendly interface for this model, which gives the results as a function of downwind distance from the source.

The equation to calculate the concentration of pollutant at distance  $x$  from the emission source in the wind direction, at ground level ( $y = 0, z = 0$ ) is [1, 3–6]:

$$C(x, 0, 0) = \frac{Q}{\pi \cdot \sigma_y \cdot \sigma_z \cdot u} \cdot \exp \left[ -\frac{1}{2} \left( \frac{H}{\sigma_z} \right)^2 \right] \left[ \frac{g}{m^3} \right] \quad (1)$$

where:  $Q$  (g/s) is the emission rate,  $\sigma_y, \sigma_z$  (m) are the dispersion coefficients,  $u$  (m/s) is the wind speed,  $H = h + \Delta h$  (m) is the effective stack height,  $h$  (m) is the built stack height,  $\Delta h$  (m) is the plume rise.

The emission plume rises from the stack due to forces: momentum determined by the impulse of the emission flux oriented vertically with a certain speed and buoyancy determined by the temperature difference between the warmer stack emission (with lower density) and atmospheric air, which leads to an ascending force [4].

To establish the dominant mechanism of plume rise (buoyant or momentum), if the temperature of the emission gas is equal or greater than the air temperature, the EPA dispersion models require the calculation of the crossover temperature difference  $(\Delta T)_c$  by [3, 4]:

$$(\Delta T)_c = 0.0297 \cdot T_s \cdot \frac{v^{\frac{1}{3}}}{d^{\frac{2}{3}}} \text{ (K)}, \text{ for } F_b < 55 \frac{m^4}{s^3} \quad (2)$$

$$(\Delta T)_c = 0.00575 \cdot T_s \cdot \frac{v^{\frac{2}{3}}}{d^{\frac{1}{3}}} \text{ (K)}, \text{ for } F_b \geq 55 \frac{m^4}{s^3} \quad (3)$$

where:  $T_s$  (K) is emission gas temperature,  $v$  (m/s) is emission gas velocity,  $d$  (m) is stack inside diameter. The buoyancy flux is calculated as follows [3–5]:

$$F_b = g \cdot v \cdot d^2 \cdot \frac{T_s - T_a}{4 \cdot T_s} \left( \frac{m^4}{s^3} \right) \quad (4)$$

where:  $g$  ( $\frac{m}{s^2}$ ) is acceleration due to gravity,  $T_a$  (K) is air temperature.

If  $\Delta T = T_s - T_a \geq (\Delta T)_c$  the plume rise mechanism is buoyant, but if  $\Delta T = T_s - T_a < (\Delta T)_c$ , the plume rise mechanism is by momentum.

The momentum flux  $F_m$  is given by [3–5]:

$$F_m = v^2 \cdot d^2 \cdot \frac{T_a}{4 \cdot T_s} \left( \frac{m^4}{s^2} \right) \quad (5)$$

The maximum ground-level concentration can be reached at great distances from the emission source. In the vicinity of the source, the ground concentration is zero due to the high altitude at which the emission is made and the air currents that carry the pollutants [7, 8]. At very long distances from the source, the pollutant concentration tends to zero as a result of dispersion. The expected variation of pollutant concentration at ground level is shown in Figure 1 where the maximum value ( $C_{max}$ ) is reached at the distance  $x_{max}$ . [7].

This study aims to estimate, using Screen View software, the PM concentration at ground level using data from stack emissions from a cement factory during 11 months (February to December) in the year 2019 [9]. Meteorological conditions about air temperature, wind direction and speed over the 11 months were collected from online data of an air monitoring station near the factory [10].

## 2. CASE STUDY

The initial parameters needed for the Screen 3 model are given in Table 1. All values are taken as averages over each season of 2019, i.e. winter (months February and March), spring (months April, May, and June), summer (months July, August, and September), and autumn (October, November, and December [9, 10].

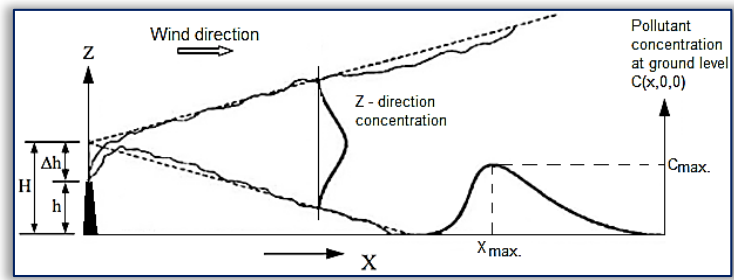


Figure 1. Gaussian plume parameters and expected pollutant concentration variation [7]

Table 1. Initial parameters for Screen 3 model [9, 10]

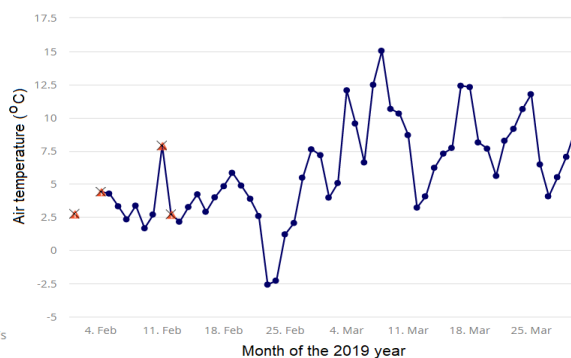
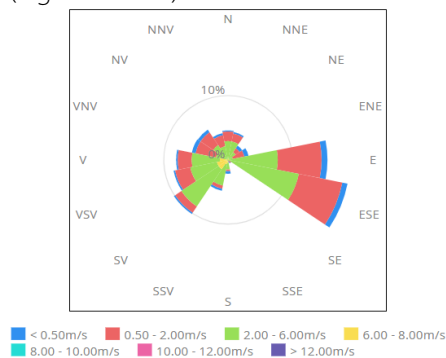
Parameter	Average values corresponding to 2019 year seasons			
	Winter (Months 2, 3)	Spring (Months 4, 5, 6)	Summer (Months 7, 8, 9)	Autumn (Months 10, 11, 12)
Emission gas temperature, (°C)	148.85	155.12	161.09	170.15
Emission gas velocity, (m/s)	10.53	10.73	11.09	10.54
Emission gas flow rate, (m <sup>3</sup> /h)	429882.37	438190.87	452894.42	430287.11
PM concentration in emission gas, (mg/ m <sup>3</sup> )	7.8030	7.4183	11.3140	8.6215
PM emission rate, (g/s)	0.9318	0.9029	1.4234	1.0305
Air temperature, (°C)	6.21	16.41	20.47	9.56
Wind speed, (m/s)	2.6	2.2	2.1	2.1

Emission parameters (temperature, flow rate, and PM concentration in emission gas) were recorded at a point source, i.e. the stack of a cement factory [9]. The emission gas velocity (in m/s) was calculated as the ratio between the emission gas flow rate in (m<sup>3</sup>/s) and the transversal area of the stack in (m<sup>2</sup>) knowing the geometrical parameters of the stack (height of 90 m and diameter of 3.8 m [9]).

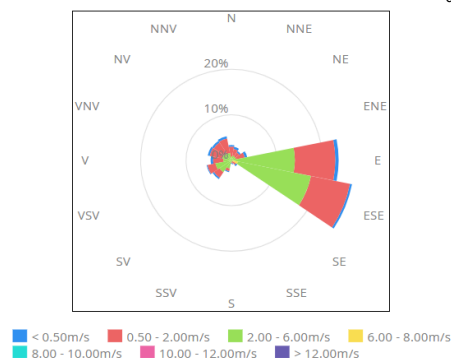
The PM emission rate was calculated (see values in Table 1) from the following relation and given in (g/s) [11]:

$$\text{PM concentration} \left( \frac{\text{mg}}{\text{m}^3} \right) = \frac{\text{PM emission rate} \left( \frac{\text{mg}}{\text{s}} \right)}{\text{Emission gas flow rate} \left( \frac{\text{m}^3}{\text{s}} \right)} \quad (6)$$

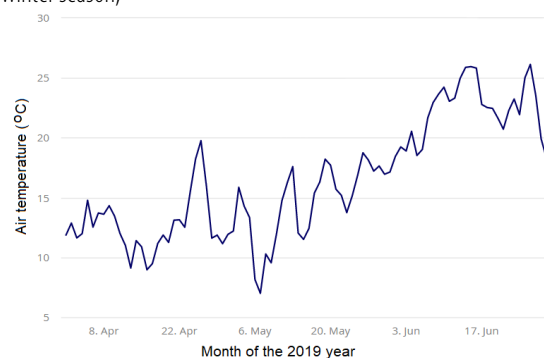
In Figures 2.a–d are shown the meteorological data (air temperature and wind rose for the direction and wind speed) recorded by an air monitoring station situated nearby the factory (BH–4) [10]. From these data, the average values of air temperature and wind speed recorded for each season were estimated are given in Table 2. The wind roses show that throughout the year 2019, the predominant wind blowing direction was east and south–east (Figures 2.a–d).



a) winter season;



b) spring season;



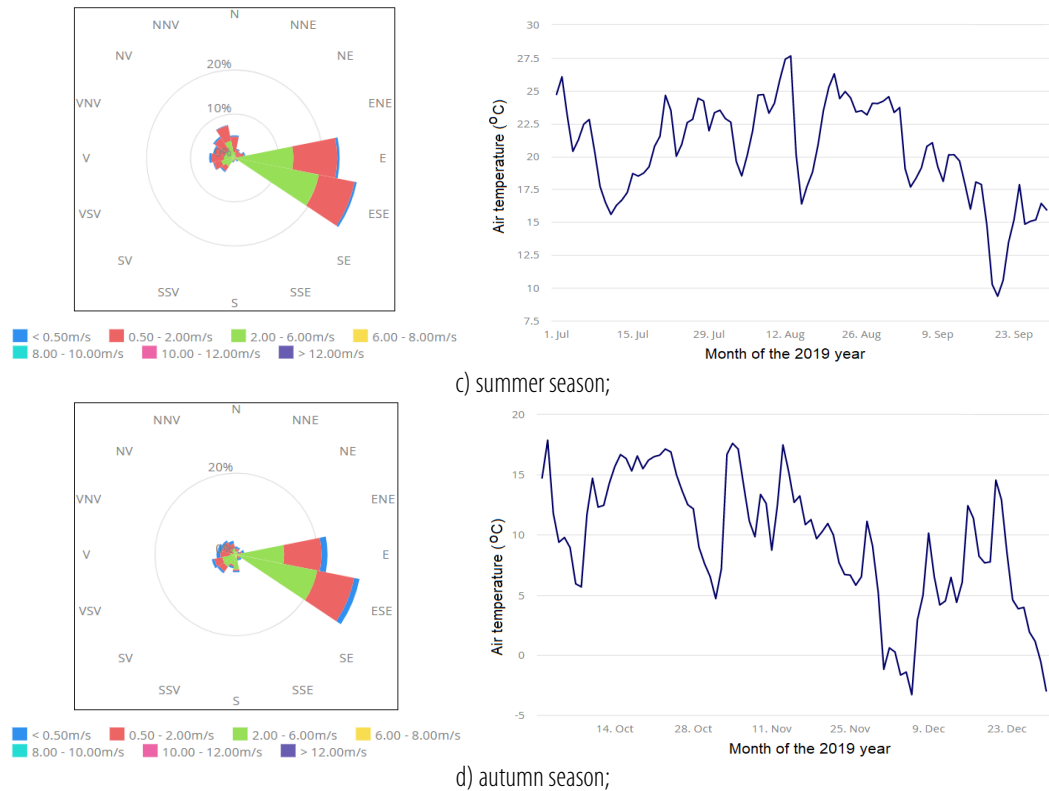


Figure 2. Meteorological data of the 2019 year seasons [10]: left, wind rose (direction and speed) and right, air temperature

In addition, in the Screen 3 model, the “flat terrain” option was chosen referring to the topography around the point source. The maximum distance from the source to estimate the PM concentration was set at 50 km, while for the dispersion coefficients the ‘rural’ conditions were set.

### 3. RESULTS AND DISCUSSION

As several initial parameters do not vary much (see values in Table 1), e.g. emission parameters (gas flow rate and velocity, PM emission rate) and wind speed, results analysis may be performed on much variable with the seasons, emission gas temperature, and air temperature. The difference between the temperature of the emission gas and the air temperature influences plume rise by buoyant or momentum mechanism and eventually the pollutant concentration at ground level [2–4, 12–14].

To evaluate the plume rise mechanism, the buoyant and momentum fluxes were estimated by the Screen 3 model for the considered periods and given in Table 2. As is the case, for  $F_b \geq 55 \frac{m^4}{s^3}$ , the relation (3) was used to calculate

the crossover temperature difference  $(\Delta T)_c$ . Comparing the obtained value with the temperature difference  $\Delta T = T_s - T_a$  resulted that predominant mechanism for the plume rise is by buoyancy.

Analyzing the values of  $F_b$  from Table 2 one may observe that the smallest value is estimated in summer (125.005  $m^4/s^3$ ) while the biggest is estimated in autumn (140.642  $m^4/s^3$ ). Otherwise, the smallest estimated value of the momentum flux  $F_m$  is in winter, while the biggest is in summer with direct dependence on the emission gas velocity value of 10.53 m/s and 11.09 m/s respectively (Table 1).

Figures 3–6 show the estimated variations of PM concentration at ground level, along the centerline of the plume, during the considered periods. Differences can be observed in terms of maximum concentration, in ( $\mu g/m^3$ ) and the corresponding downwind distance from the stack, in (m).

Among the obtained results (Figures 3–6), minimum PM concentration of 0.1379  $\mu g/m^3$  is estimated in the autumn season of 2019 (Figure 6), while the maximum estimated value of 0.2167  $\mu g/m^3$  is estimated in the summer season of 2019 (Figure 5). The indirect dependence with corresponding buoyant fluxes is evident, i.e. in summer the calculated value of  $F_b$  is minimal, while for the autumn season it is maximal (see values in Table 2). This indirect dependence is explained by the increase of the buoyant flux value that increases floatability of the plume in air, so the pollutant concentration at ground level is expected to decrease [13, 15].

Table 2. Screen 3 estimations of buoyant and momentum fluxes for the 2019 seasons

2019 season	Buoyant flux $F_b$ ( $m^4/s^3$ )	Momentum flux $F_m$ ( $m^4/s^2$ )
winter	132.563	288.109
spring	126.465	294.949
summer	125.005	296.587
autumn	140.642	279.046

CALCULATION MAX. CONC. DIST. TO TERRAIN  
 PROCEDURE ( $\mu\text{g}/\text{m}^3$ ) MAX. (m) HT (m)

-----  
 SIMPLE TERRAIN 0.1568 14432 0

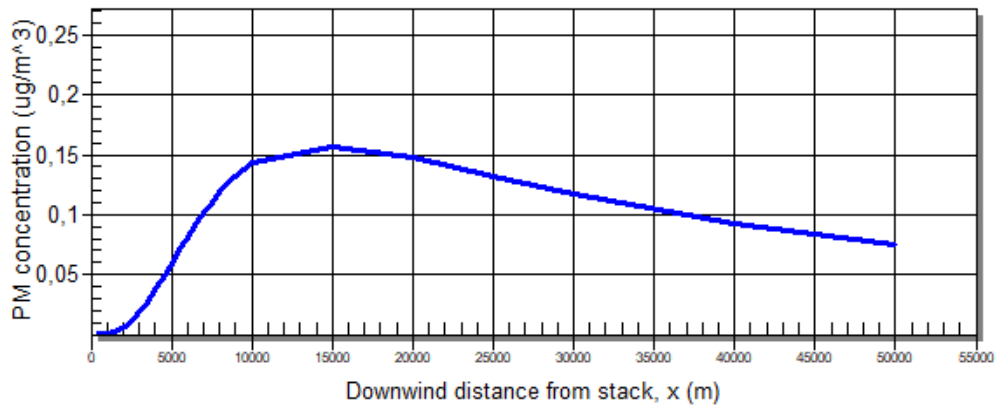


Figure 3. Variation of PM concentration along plume centerline, winter season of 2019

CALCULATION MAX. CONC. DIST. TO TERRAIN  
 PROCEDURE ( $\mu\text{g}/\text{m}^3$ ) MAX. (m) HT (m)

-----  
 SIMPLE TERRAIN 0.1409 16913 0

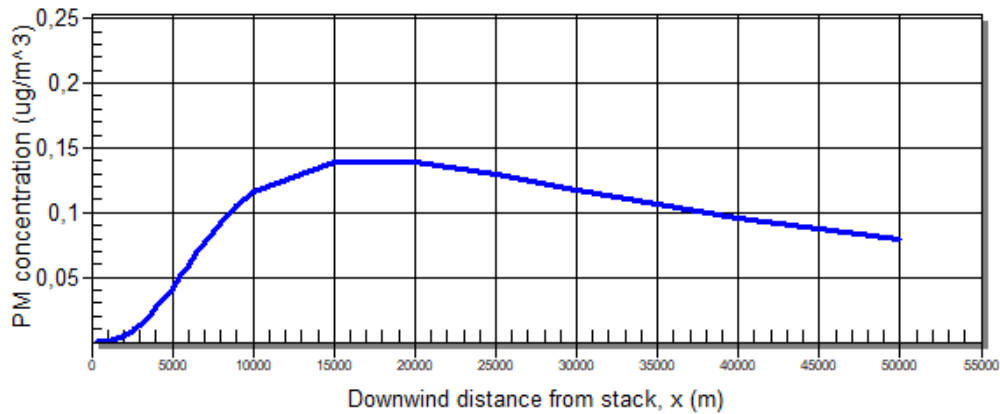


Figure 4. Variation of PM concentration along plume centerline, spring season of 2019

CALCULATION MAX. CONC. DIST. TO TERRAIN  
 PROCEDURE ( $\mu\text{g}/\text{m}^3$ ) MAX. (m) HT (m)

-----  
 SIMPLE TERRAIN 0.2167 17710 0

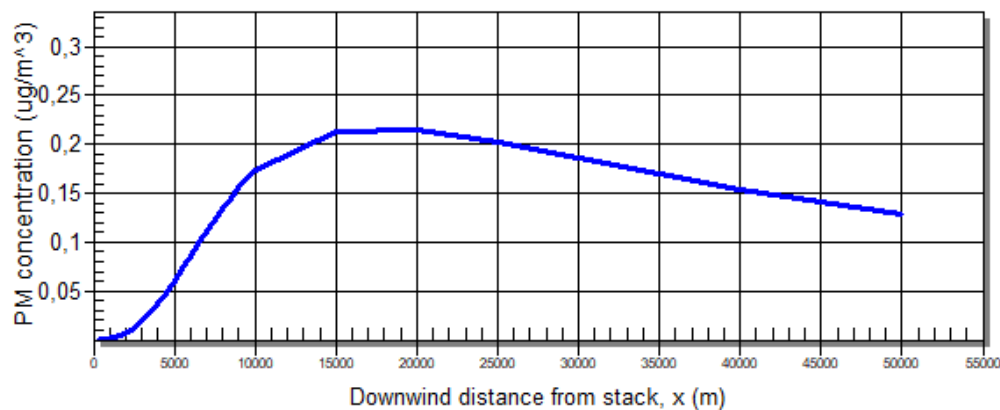


Figure 5. Variation of PM concentration along plume centerline, summer season of 2019

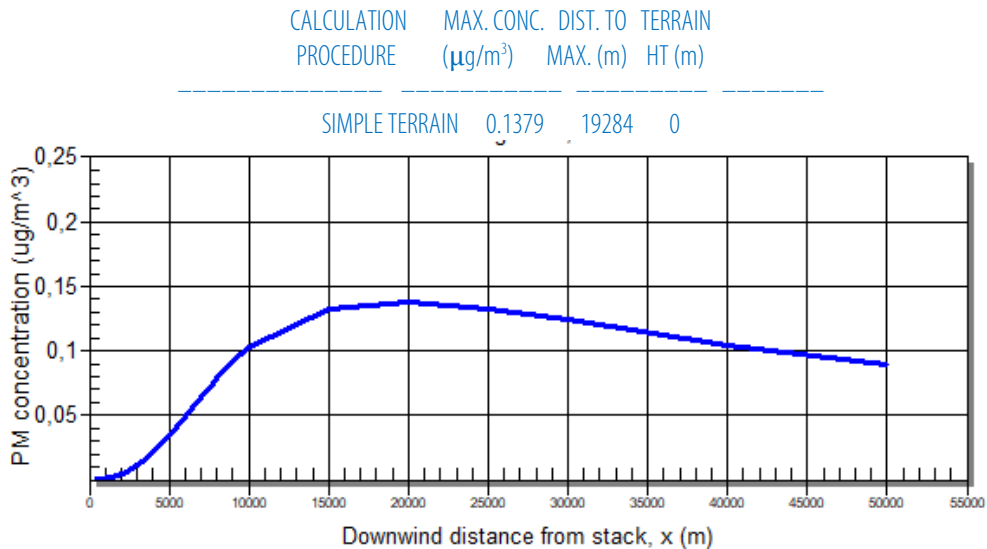


Figure 6. Variation of PM concentration along plume centerline, autumn season of 2019

For the winter season, the estimated maximum PM concentration at ground level is of  $0.1568 \mu\text{g}/\text{m}^3$  (Figure 3), while for the spring season the estimated value is  $0.1409 \mu\text{g}/\text{m}^3$  (Figure 4).

#### 4. CONCLUSIONS

This study presents quantitative results obtained by the Screen 3 model in terms of PM concentration variations estimated at ground level after a point source emission during 11 months over the year 2019. Initial emission parameters were classified in four seasons (winter, spring, summer, and autumn) including the months in which the experimental measurements were made [9]. The model was completed with meteorological data measured by an air monitoring station located near the point emission source [10]. In conclusion, the estimated values PM concentration were correlated with estimated buoyant flux values, which was shown that it is the main mechanism of plume rise.

#### References

- [1] Lakes Environmental. Screen View User's Guide. Canada; 1995.
- [2] Khaniabadi YO, Sicardb P, Taiwoc AM, De Marcod A, Esmaelie S, Rashidi R. – Modeling of particulate matter dispersion from a cement plant: Upwind–downwind case study, *Journal of Environmental Chemical Engineering* 2018;6:3104–10.
- [3] USEPA – U.S. Environmental Protection Agency– SCREEN3 Model User's Guide, EPA–454/B–95–004; North Carolina: Office of air quality; 1995.
- [4] USEPA – U.S. Environmental Protection Agency– User's guide for the industrial source complex (ISC3) dispersion models for use in the multimedia, multipathway and multireceptor risk assessment (3MRA) for HWIR99, Volume II: description of model algorithms. Washington: Office of Research and Development; 1999.
- [5] Ujoh F, Ifatimehin OO, Kwabe ID – Estimating Plume Emission Rate and Dispersion Pattern from a Cement Plant at Yandev, Central Nigeria. *Resources and Environment* 2014;4:115–38.
- [6] Baroutian S, Mohebbi A, Soltani Goharrizi A. – Measuring and modeling particulate dispersion: A case study of Kerman Cement Plant, *Journal of Hazardous Materials* 2006;136:468–74.
- [7] Weiner RF, Matthews R. – Environmental engineering. Fourth edition, Butterworth–Heineman, UK: Elsevier Science; 2003.
- [8] Ciobanu C, Istrate IA, Tudor P, Voicu G. – Dust Emission Monitoring in Cement Plant Mills: A Case Study in Romania, *International Journal of Environmental Research and Public Health* 2021;18,9096:1–16.
- [9] Heidelberg Cement Romania – Annual environment report of the cement factory [Internet]. 2019 [cited 2022 February 10]. Available from: <https://www.heidelbergcement.ro/ro>.
- [10] RNMCA – National Network for Monitoring Air Quality, Romanian Ministry of Environment [Internet]. 2019 [cited 2022 February 10]. Available from: [https://www.calitateaer.ro/public/monitoring–page/reports–reports–page/?\\_\\_locale=ro](https://www.calitateaer.ro/public/monitoring–page/reports–reports–page/?__locale=ro).
- [11] Varma SAK, R. Humar M, Kumar AB. Emissions Inventory and Emission Factors for Cement Industry, *International Journal of ChemTech Research* 2017;10:402–8.
- [12] Flori M, Miloştean D. – Mathematical analysis of air pollution from stacks using Briggs method, *Annals of Faculty Engineering Hunedoara – International Journal of Engineering* 2020;4:145–48.
- [13] Keawboonchu J, Malakan W, Thongkum W, Thepanondh S. – Effect of the Waste Heat Recovery System to Buoyancy and Momentum Flux of Combustion Stack in the Cement Industry, *Environment and Natural Resources Journal* 2018;17:11–21.
- [14] Amah VE, Udeh N, Effiong BO. – Particulate Matter Pollution around a Cement Industry and its Potential Effect, *Journal of Scientific Research and Reports* 2020;26:130–40.
- [15] Abu–Allaban M, Abu–Qudais H. – Impact Assessment of Ambient Air Quality by Cement Industry: A Case Study in Jordan, *Aerosol and Air Quality Research* 2011;11:802–10.